

Environmental Progress & Sustainable Energy

An assessment on removal performance of Arsenic with treated *Turbinaria vulgaris* as an adsorbent: characterization, optimization, isotherm and kinetics study

Journal:	<i>Environmental Progress</i>
Manuscript ID	Draft
Wiley - Manuscript type:	Original Manuscript
Date Submitted by the Author:	n/a
Complete List of Authors:	Khan, Anoar; Vignan University, chemical Engineering; National Institute of Technology, Chemical Engineering Boddu, Sumalatha; Vignan University, Chemical Engineering Department Dulla, John; Vignan University, Department of Biotechnology Alugunulla, Venkatanarayana; Vignan University, Department of Biotechnology
Keywords:	Biosorption, Arsenic, Isotherm, Kinetics, Optimization
Alternate Keywords:	T. vulgaris, RSM, Characterization

SCHOLARONE™
Manuscripts

Highlights

- Surface characteristic of Treated *T. vulgaris* evidenced as a better As removal biosorbent
- Maximum As metal uptake has been attained to 26.54 mg/g with removal efficiency of 92.12%
- *T. vulgaris* could be a suitable biosorbent over wide range of pH and As concentration
- Five various kinetic model and four isotherm study has been completed during removal study
- Kinetics and isotherm study shows that *T. vulgaris* could be an efficient biosorbent

1
2
3 1 **An assessment on removal performance of Arsenic with treated *Turbinaria vulgaris* as an**
4 2 **adsorbent: characterization, optimization, isotherm and kinetics study**

5
6
7 3 **Sumalatha B¹, John babu D², A. Venkatanarayana², Anoar Ali Khan^{1*}**

8
9 4 ¹Chemical Engineering Department, VFSTR deemed to be University, Vadlamudi, India

10 5 ²Department of Biotechnology, VFSTR deemed to be University, Vadlamudi, India
11 6
12 7
13 7
14 7

15 8 **Abstract**

16
17 9 In this current research, batch experiments were performed towards the characterization and
18 optimization of arsenic removal by *Turbinaria vulgaris* (*T.vulgaris*). The four process
19 parameters i.e. initial solution pH (3–5), initial arsenic ion concentration (20–100 mg/l),
20 *T.vulgaris* dosage (0.1–0.5 g/L) and temperature (293-313K) were considered for the process
21 optimization through response surface methodology (RSM) via central composite design (CCD)
22 approach. According to CCD methodology a set of 30 experimental runs were conducted and the
23 results were analysed, suggested quadratic model has well matched to the experimental results
24 which might be used to design space according to ANOVA study. The highest removal efficiency
25 of 92.12% was attained, retaining the process conditions viz. pH 4.41, biomass dosage 0.3 g/L
26 and initial arsenic concentration 21.33 mg/L and temperature 298.32 K. Biosorbent morphology
27 and chemical properties were characterized by means of FT-IR and SEM analysis. The presence
28 of metal ions in the *T.vulgaris* biomass after biosorption was confirmed from SEM result. These
29 results are significant towards the assessment and optimization of removal of arsenic ions by
30 *T.vulgaris* biomass. To estimate the solute interaction and bio-sorption nature, the experimental
31 data were verified with different isotherms and kinetic models. The results discovered that
32 *T.vulgaris* could be a cost-effective and eco-friendly bio-sorbent for removal of arsenic ions.
33
34
35
36
37
38
39
40
41
42
43
44
45

46 26 **Keywords:** Bio-sorption; RSM; Arsenic; *T.vulgaris*; Isotherms; Kinetics.
47
48
49

50 28 *Corresponding author

51 29 Email address: anoaralikhan@gmail.com
52
53
54
55
56
57
58
59
60

1. Introduction

Gradual escalation of heavy metal pollution in aqueous environment experienced an immense concern in the second half of 20th century, since the occurrence of many industrial and environmental accidents, warned the world for the sake of harmful environmental consequences. A huge attention of researchers and authorities has been motivated towards arsenic (As), as it has been projected as an influential element towards the impact on environmental pollution related to heavy metal throughout the world since last few decades. Arsenic is a metalloid, having properties of metals and non-metals; known to be carcinogenic to humans, is persisting in environment through various industrial activities and anthropogenic sources [1]. Researchers have been focused on the potential research on heavy metal pollution as well as the influence on human health and environment through inspection of arsenic abundance, behaviour and remediation. The World Health Organization (WHO) has established the guidelines of permissible limit of arsenic in drinking water as 10µg/l, since 2006 [2]. This has become the motivation for removal of arsenic during last few decades using various technologies, amongst them biosorption turn out to be a popular one due to high adsorption capacities, low costs and regeneration characteristics. Due to its efficient sorption of many contaminants and the detoxification property of heavy metals in human body, algae have been introduced and were used to remove heavy metals from industrial wastewaters. This has been the major reason behind the use of various strains of algae for wastewater treatment since last few years [3, 4, 5, 6]. *Turbinaria vulgaris* has been considered as one of the potential algae that could be used to remove the heavy metal contamination from wastewater.

The biosorption mechanism has become more complex and non-linear due to the presence of various biological components in metal removal. Optimization of process parameters is essential

1
2
3 55 to maximize the biosorption efficiency and to make the process as economically viable. The
4
5 56 classical method of optimization has certain disadvantages like ignorance of interaction effect,
6
7 57 requirement of more experimental runs, etc. Therefore, the use of classical “one factor at a time”
8
9
10 58 method is not advisable for the optimization of non-linear processes. In order to overcome the
11
12 59 problem of multivariate optimization, various statistical tools have been employed to find out the
13
14 60 optimum combination and interaction of process parameters. Factorial design and RSM were
15
16 61 considered as the most popular designs used for the optimization of multivariable processes [7].
17
18 62 In the present study, the pretreated *T.vulgaris*. (brown algae) was used as biosorbent for efficient
19
20 63 removal of arsenic from an aqueous solution. The objective of the present investigation focuses
21
22 64 on the optimization of process variables for optimum arsenic removal, isotherm studies and
23
24 65 estimation of biosorption kinetics of arsenic with possible mechanism.
25
26
27

28 66 **2. Materials and Methods**

29 67 **2.1. Preparation of biomass**

30
31
32
33 68 The biosorbent, *T.vulgaris* used in the present study was gathered from the Gulf of Mannar,
34
35 69 Tamil Nadu, India. The collected algae was washed with deionized water several times to get rid
36
37 70 of unwanted material. The washing procedure was kept till the wash water contains no dirt. The
38
39 71 washed *T.vulgaris* was completely dried and scorching it for about 3-4 weeks. The dried leaves
40
41 72 then crushed into small pieces and make in powdered form using domestic mixer. The prepared
42
43 73 *T.vulgaris* was pre-treated using 0.1 M CaCl_2 which increases the active sites and surface
44
45 74 firmness of dry adsorbent. In order to modify algae, 20 g of dried algae was shed in 200 ml
46
47 75 CaCl_2 0.1 M solution and stirred for 24 h with a stirring agitator at a speed of 200 rpm.
48
49
50
51 76 Afterward, the solution was filtered using Whatman filter paper and algae were washed with
52
53
54
55
56
57
58
59
60

77 doubled distilled water and kept in the oven at 343.14 K for 48 h. In the present study, the
78 powdered materials have an average particle size range of 75-212 μm .

79 **2.2. Preparation of stock solution**

80 Arsenate solution was prepared by dissolving solid $\text{Na}_2\text{HAsO}_4 \cdot 7\text{H}_2\text{O}$ in distilled water. The ionic
81 strength of solutions was adjusted by addition of (0.1N) HNO_3 and (0.1N) NaOH .

82 **2.3. Bio-sorption Experiments:**

83 Arsenic removal capacity of *T.vulgaris* was investigated by varying the pH, initial concentration
84 of arsenic ions, biomass dosage and temperature at a constant volume of reaction mixture, 30 ml
85 designed from CCD. The samples were agitated at 180 rpm for a pre determined contact time of
86 60 min (not discussed here) and filtered using Whatman 40 filter paper. The Atomic Absorption
87 Spectroscopy (Shimadzu AA 6300) was used to evaluate the presence of residual arsenic in
88 solution. To ensure the presence of the arsenic in the solution blank and triplicate experiments
89 were conducted and the mean values have been recorded.

90 The metal uptake of arsenic onto *T.vulgaris* was determined from the accompanying
91 mathematical expression.

$$92 \quad q = \frac{V(C_i - C_f)}{1000w} \quad (1)$$

93 Where q signifies the amount of arsenic biosorbed by *T.vulgaris* (mg/g), C_i is the initial
94 concentration of solute in the solution before biosorption (mg/l), C_f indicates the final
95 concentration of solute in the solution after adsorption (mg/l), V is the volume of the metal
96 solution and w is the mass of *T.vulgaris*.

97 2.4. Central composite design (CCD)

98
99 In order to develop the empirical relation between the process variables and response, a standard
100 experimental design of RSM called the Central composite design (CCD) is used. The
101 experimental design matrix for four variables and each with three levels (-1, 0, +1) is designed
102 by CCD in order to find out the optimum values of pH, metal ion concentration, biomass dosage
103 and temperature. The ranges and levels of independent process parameters are given in Table.1.
104 The mathematical equation relating four independent process variables and the response function
105 i.e., percentage removal of metal ions has been expressed by the following quadratic model.

$$106 \quad Y = \beta_0 + \beta_1 A + \beta_2 B + \beta_3 C + \beta_4 D + \beta_{11} A^2 + \beta_{22} B^2 + \beta_{33} C^2 + \beta_{44} D^2 + \beta_{12} AB + \\ 107 \quad \beta_{13} AC + \beta_{23} BC + \beta_{14} AD + \beta_{24} BD + \beta_{34} CD \quad (2)$$

108 Where, Y indicates predicted response, β_0 the intercept term, β_i the linear effect, β_{ii} the standard
109 effect and β_{ij} the interaction effect.

110 2.5. Equilibrium models

111 2.5.1. Langmuir & Freundlich Isotherms

112 In order to predict maximum arsenic removal by *T.vulgaris*, the equilibrium studies are
113 performed. Experiments were conducted at 20mg/l by fixing other parameters as constant.
114 Langmuir and Freundlich models were used in establishing equilibrium relation between the
115 biosorbed arsenic ions by *T.vulgaris* (q_e) and residual arsenic ions in solution (c_e). Langmuir
116 isotherm has been extensively used for dilute solutions in following linear form[8].

$$117 \quad \frac{C_e}{q_e} = \left(\frac{C_e}{a}\right) + \frac{1}{ab} \quad (3)$$

1
2
3 118 where, 'a' represents maximum metal uptake per unit mass of adsorbent to form complete
4
5 119 monolayer and 'b' represents the affinity of binding sites. The plot of (c_e/q_e) against (c_e) indicates
6
7
8 120 the applicability of this model. From the graph, it has seen that, the equilibrium data was well
9
10 121 fitted by Langmuir model.

11
12
13 122 Freundlich model can be described by the below mentioned equation [9]

$$14 \quad 123 \quad q_e = K_f C_e^{1/n} \quad (4)$$

15
16
17
18
19
20 124 where, the value of k_f and n are indicators of biosorption capacity and intensity respectively. The
21
22 125 linear plot of $\log(q_e)$ against $\log(c_e)$ describes the fitness of this model.

23 24 25 126 *2.5.2. Dubinin–Radushkevich (D-R) isotherm*

26
27
28 127 D–R isotherm model is used to determine the nature of biosorption as physical or chemical
29
30 128 process. The linear form of this model is expressed as [10]

$$31 \quad 129 \quad \ln q_e = \ln q_m - \beta \varepsilon^2 \quad (5)$$

32
33
34 130 Where q_e and q_m are equilibrium and maximum metal uptake (mol/g) respectively, β is the
35
36
37 131 activity coefficient which represents mean biosorption energy (mol^2/J^2) and ε is the Polanyi
38
39
40 132 potential which is estimated from the following equation

$$41 \quad 133 \quad \varepsilon = RT \ln \left(1 + \frac{1}{c_e} \right) \quad (6)$$

42
43
44
45 134 The mean biosorption energy (E , kJ/mol) is calculated from

$$46 \quad 135 \quad E = \frac{1}{\sqrt{-2\beta}} \quad (7)$$

1
2
3 136 If E value is between 8 and 16 kJ/mol, the biosorption process follows chemically and if $E < 8$
4
5 137 kJ/mol, the biosorption process is a physical process. The mean biosorption energy was
6
7
8 138 calculated as 5.79 kJ/mol for the biosorption of arsenic ions.
9

10 11 139 *2.5.3. Temkin isotherm*

12
13
14 140 The Temkin isotherm model takes into account the interactions between biosorbate and
15
16 141 biosorbent species [11]. Temkin isotherm assumes that the heat of biosorption decreases linearly
17
18 142 on a surface and the molecules biosorbed over the surface are epitomized with consistent binding
19
20 143 energies up to a notable maximum value. Consequently, Temkin and Pyzhev suggested that due
21
22 144 to the effect of indirect interaction of sorbate molecules, there is a significant reduction in heat of
23
24 145 biosorption of the sorbate on the surface of the biosorbent. The linearized Temkin isotherm is
25
26 146 presented as follows:
27
28
29

$$30
31
32 147 \quad q_e = \frac{RT}{b} \ln A_T + \frac{RT}{b} \ln C_e \quad (8)$$

$$33
34
35
36 148 \quad q_e = B \ln K_T + B \ln C_e \quad (9)$$

37
38
39 149 where $B = RT/b$, b stands for Temkin constant related to heat of sorption (J/mol); A indicates
40
41 150 Temkin isotherm constant (L/mg), R signifies the universal gas constant (8.314 J/mol K), and T
42
43 151 the absolute temperature (K). A plot of q_{eq} versus $\ln C_{eq}$ enables the determination of the isotherm
44
45 152 constants K_T and b .
46
47
48
49

50 153 **2.6. Kinetic models**

51 154 52 155 *2.6.1. Pseudo-first & second order models* 53 156

1
2
3 157 The equilibrium and kinetic studies were conducted in order to find out biosorption mechanism
4
5 158 as well as several parametric determination such as; initial adsorption rate, order of metal uptake
6
7
8 159 kinetics, rate constant, rate controlling mechanism, diffusion coefficient, etc. Equation 10
9
10 160 denoted as an experimental correlation for first order kinetics [12]

$$11 \quad \ln(q_e - q_t) = \ln q_e - k_{p1}t \quad (10)$$

12
13
14
15 162 Pseudo second order equation is given by [13]

$$16 \quad \frac{t}{q_t} = \frac{1}{k_{p2}q_e^2} + \frac{t}{q_e} \quad (11)$$

17
18
19
20
21
22 164 where k_{p1} and k_{p2} signifies the pseudo first order and second order rate constants respectively. q_e
23
24 165 and q_t symbolized for metal uptake at equilibrium and uptake at time t respectively for both
25
26 166 models.

27 167 2.6.2. Intra-particle diffusion model

28
29
30
31 168 The influence of metal ion diffusion through the adsorbent pores on rate of biosorption was
32
33 169 detected and characterized by the below mentioned equation [14]

$$34 \quad q_t = K_{ip}t^{0.5} + I \quad (12)$$

35
36
37
38
39 171 Where k_{ip} indicates rate constant and I specifies intercept value which determine the boundary
40
41 172 layer thickness. The linearity plot between q_t and $t^{0.5}$ shows the acceptability of proposed model.

42 173 2.6.3. Boyd model

43
44
45
46 174 This proposed model is used to predict the slowest rate controlling of biosorption process.
47
48 175 Equation (13) represents the kinetic rate data which were investigated by Boyd model [12]

$$49 \quad F = \left(1 - \frac{6}{\pi^2}\right) \exp(-\beta_t) \quad (13)$$

1
2
3 177 Where F indicates the metal uptake relative to equilibrium uptake and β_t signifies a mathematical
4
5 178 character calculated from below mentioned equation (14).
6
7

$$8 \quad 179 \quad \beta_t = -0.4977 - (1 - F) \quad (14)$$

10
11 180 From the experimental data vs. Time plot, β_t value was determined, from which the rate
12
13 181 controlling step was also established.
14

15 182 *2.6.4. Elovich model*

16
17
18 183 Elovich equation was widely used by many researchers to demonstrate second order reaction
19
20 184 kinetics of heterogeneous reactions. This was first employed to illustrate the kinetics of
21
22
23 185 chemisorption mechanism of gas molecules onto a solid surface [15]. In recent years it had been
24
25
26 186 successfully utilized by the investigators headed for chemisorption behavior of biosorption. The
27
28 187 Elovich equation can be represented as:
29
30

$$31 \quad 188 \quad q_t = \left(\frac{1}{b}\right) \ln(ab) + \frac{1}{b} \ln t \quad (15)$$

32
33 189 Where 'a' and 'b' suggests the initial sorption rate and the constant associated with the
34
35 190 magnitude of surface coverage and required activation energy for chemisorption respectively.
36
37
38

39 191 **3. Results and Discussions**

40
41
42 192 The functional groups like hydroxyl, carboxyl, amine, sulphate and phosphate composing the
43
44 193 algal cell wall plays a major role in metal binding [16]. The FTIR spectra of *T.vulgaris* algae
45
46
47 194 were documented at the frequency range of 4000 to 500 cm^{-1} considering before and after arsenic
48
49
50 195 biosorption which shown in Fig 1. Several peaks (Fig. (1a)) were observed indicating the
51
52 196 presence of various functional groups which are responsible for binding of arsenic. The broad
53
54 197 peak at 3334.92 cm^{-1} specifies O-H stretching vibration which indicates alcohols and phenols
55
56
57
58
59
60

1
2
3 198 existence on biosorbent surface. The peaks within a stretch of 2924.09 -2852 cm⁻¹ revealed O-
4
5 199 H,C-H and N-H bonds, which imply carboxylic and amino groups [16]. In most of the brown
6
7
8 200 algae, 70% of cell wall functional groups are carboxylic and amino groups, these groups play
9
10 201 vital role in metal binding [17]. The peaks at wave numbers of 1616.35, 1317.38, 1246.02,
11
12 202 1066.64, 1037.7, 781.17 and the peaks below 500 cm⁻¹significantly indicates the presence of N-
13
14
15 203 H, C-O, C-N, C=C,C-F, C-Cl and C-I groups respectively [16]. Therefore, the surface functional
16
17 204 groups of a cell wall like carboxylic acids, amino, alkenes and alkyl groups are responsible for
18
19 205 biosorption of arsenic. Comparison of FTIR spectra of *T.vulgaris* with arsenic (Fig. (1b))
20
21 206 revealed the significant changes. One indication of chemical reaction between metal ions and
22
23
24 207 surface functional groups concluded from apeak appearance at 3365.78 cm⁻¹ and disappearance
25
26 208 at 3334.92 cm⁻¹. The absorption peaks of C-H &O-H stretching vibrations marginally moved
27
28 209 from 2924.09 to 2926.01 cm⁻¹. The shift of C-O stretch from 1317.38 to 1319.31 cm⁻¹ point out
29
30
31 210 the strong association of carboxylic acids, esters and aldehydes through biosorption process[18].
32
33 211 The swing of peak from 1157.28 to 1103.28 cm⁻¹shows the contribution of more alcoholic
34
35 212 groups in biosorption process. On comparision of the IR spectra of *T. vulgaris* before and after
36
37
38 213 biosorption, it is seen that bisorption bands shifted to higher values due to carboxylate and
39
40 214 hydroxylate anions.

41
42
43 215 In order to study the surface texture and porosity of biosorbent the SEM analysis of *T.vulgaris*
44
45 216 was performed. The result obtained is shown in Fig.(2a). It clearly illustrates that the surface area
46
47
48 217 of *T. vulgaris* is highly heterogeneous and uneven with porous structure. The SEM micrograph
49
50 218 of *T. vulgaris* showed that the biosorbent is highly heterogeneous and the surface morphology of
51
52 219 biosorbent is rough. SEM micro graphs of biosorbent *T.vulgaris* after biosorption of arsenic is
53
54
55 220 shown in Fig.(2b). The surface of metal loaded biosorbent clearly shows that the surface of

221 biosorbent dosage was covered with metal ions. The pores was completely filled with the metal
 222 ions after the biosorption of arsenic metal and the pores appear to be smooth which indicates that
 223 the metal was biosorbed to the functional groups present in the pores. The surface of the
 224 biosorbent became smooth after the biosorption of arsenic metal.

225 3.2. Optimization of process parameters

226 3.2.1. Response surface methodology

227 A quadratic model has been established via CCD approach considering the process variables viz.
 228 pH (A), initial concentration (B), biosorbent dosage (C) and temperature. Overall 30
 229 experimental runs was planned which comprises of 16 factorial, eight axial and six centre points
 230 were performed along with analysis of obtained results. A design matrix created using CCD with
 231 implicit variables, response reported from experiments and predicted response for biosorption of
 232 arsenic onto *T.vulgaris* is given in Table 2.

233 3.2.2. Regression analysis

234 The following reduced quadratic model equation represents an empirical correlation between the
 235 response (sorption percentage of arsenic) and input variables in coded terms established by RSM
 236 software:

$$237 (Y) = 86.63 + 6.11 A - 4.6 B + 1.7 C - 1.09D - 21.24A^2 - 0.49 B^2 - 0.41C^2 - 0.54D^2 - 0.93AB - 1.67AC \\ 238 + 8.125 \times 10^{-3}AD + 1.3BC + 0.49BD + 0.18CD \quad (16)$$

239 The influence of individual variables on the biosorption of arsenic from an aqueous solution
 240 represented by equation (16) and noted that factors A and C had a proportional impact, whereas

241 B and D gave a negative effect on biosorption of arsenic. Similar trends of results were specified
242 for biosorption of chromium onto chitosan and carbonized rice husk [18].

243 3.2.3. *Fitting the quadratic model*

244 The statistical significance of the quadratic model was evaluated by the analysis of variance
245 (ANOVA) as presented in table 3. The results showed that this regression was statistically
246 significant at F-value of 352.88 and lack of fit tests clearly specifies the model and insignificance
247 of lack of fit confirms the model suitability.

248 Besides significant “model P-value” (< 0.0001), large “lack of fit P-value” (0.2071) and higher
249 determination coefficient (0.997) also confirms the significance of model. Effect of individual
250 parameters and their interaction was examined using P-values of respective factor i.e. A, B, C, D,
251 AB, AC, BD, A^2 [18]. Collaborative effect of pH and initial concentration, pH and biosorbent
252 dosage, initial concentration and biosorbent dosage have more significant influence as compared
253 to individual variable such as pH, initial concentration, biosorbent dosage and temperature.
254 Square effect of pH had also indicates moderate significance on biosorption. Entire ANOVA
255 studies point out, the model acceptability of biosorption process through simulation of arsenic
256 removal by means of *T. vulgaris*.

257 3.2.4. *Optimization of process variables and authentication*

258 After the development of the mathematical model for the biosorption of arsenic onto *T. vulgaris*,
259 optimization was carried out to predict the maximum metal uptake by *T. vulgaris*. Predicted
260 solution by RSM is shown as contour plot in Fig.3. Through RSM model, at a fixed optimum
261 conditions of pH 4.1, initial concentration of 22.81 mg/l, biosorbent dosage of 0.49 mg/l and
262 temperature 298.32 K, projected a maximum 92.12% removal of arsenic via biosorption. A new

1
2
3 263 experiment was conducted to assess the validity of optimization of process using RSM,
4
5 264 considering the optimum parametric condition. 92.02% arsenic removal is attained thru the
6
7 265 current study which is extremely well likened to RSM model predicted value. Therefore the
8
9
10 266 model projected conditions specified by RSM were selected as optimum removal parameters of
11
12 267 arsenic via biosorption through *T.vulgaris*.

15 268 3.2.5. Interactive effects of two variables

18 269 The combined effects of process variables on biosorption were analyzed with the help of 3D
19
20 270 (three dimensional) surface diagram. Fig. (4a) illustrates the combined influence of initial metal
21
22 271 ion concentration and initial pH of the solution and noticeably point out the supremacy of pH
23
24 272 over initial concentration. An increase in initial concentration experienced a rise in sorption
25
26 273 percentage instead of decline result. In overall the effect of initial metal ion concentration was
27
28 274 decreased by the effect of pH. Fig. (4b) represents the interactive impact of pH and bio sorbent
29
30 275 dosage on arsenic removal and clearly shows the superiority of pH over biosorbent dosage. The
31
32 276 sorption percentage of arsenic was greater at higher biosorbent dosage because of more binding
33
34 277 sites, increase in negative charge on biosorbent surface along with an increase of pH, both
35
36 278 collectively provided increase of biosorption percentage. The interactive effects of temperature
37
38 279 and pH is shown if Fig. (4c) and observed that increase in tendency of sorption percentage
39
40 280 initially and then decreased with increasing temperature. The interactive effects of the biosorbent
41
42 281 dosage and initial metal ions concentration canbe inferred from the response plot of Fig. (5a)
43
44 282 holding pH at central values. From the figure it could be observed that percentage biosorption
45
46 283 was increased with increase in dosage and percentage biosorption was increased with decrease in
47
48 284 initial concentration, which concludes the significant impact of both the variables. The
49
50 285 interactive effects of temperature and initial concentration are shown in Fig. (5b) and clearly

1
2
3 286 shows the percentage biosorption was increased with increase in temperature. Considering
4
5 287 overall effect, percentage biosorption was decreased with increasing concentration. The
6
7 288 interactive effects of temperature and dosage are shown in Fig. (5c). It clearly indicates that with
8
9
10 289 increase in dosage the percentage biosorption increased and sorption percentage was decreased
11
12 290 with increasing temperature. Similar results were obtained for lead removal by a novel super
13
14 291 paramagnetic nanocomposite [19]. It can be verified from ANOVA study that, the p-value of the
15
16 292 factor AD, BD, CD is very high, which indicates the insignificant effect of those factor. From
17
18 293 the experimental and graphical analysis concludes that, collaborative impact of pH and
19
20 294 temperature, initial concentration and temperature, biosorbent dosage and temperature had no
21
22 295 such significant influence on arsenic biosorption.
23
24
25
26

27 296 **3.3. Isotherm studies**

28
29
30 297 The equilibrium sorption data was tested by fitting the experimental data on the Langmuir,
31
32 298 Freundlich, D-R, Temkin models towards knowing the sorption isotherm. The Langmuir
33
34 299 mathematical model is used to estimate the maximum adsorption capacity conforming to the
35
36 300 complete monolayer scope on the biosorbent surface. Thereby, the Langmuir isotherm represents
37
38 301 the equilibrium distribution of metal ions between the solid and liquid phases. In Fig. (6a), $C_{eq} /$
39
40 302 q_{eq} was plotted against C_{eq} yielding a straight line with $R^2 = 0.996$ for arsenic signifies that
41
42 303 sorption data were well matched with Langmuir model. From slope of the linear plot, (Q_{max}
43
44 304 $= 25.64$ mg/g) value for arsenic was determined, where as $K_L = 0.1029$ value was derived from
45
46 305 the intercept.
47
48
49
50
51
52

53 306 **3.3.1. Freundlich isotherm**

1
2
3 307 Logarithmic plot of adsorbed and equilibrium concentration provides a straight line with
4
5 308 coefficient of determination close to unity (0.984 for arsenic). The values of $1/n$ (0.493 for
6
7
8 309 arsenic) and K_f (3.724 for arsenic) are originated from the slope and intercept of the straight
9
10
11 310 line for arsenic and chromium respectively which is shown in Fig. (6b) and tabulated in Table 4.

12
13
14 311 The magnitude of K_f and n indicates an easy separation of arsenic ions from an
15
16
17 312 aqueous solutions with high biosorptive capacity of the *T. vulgaris*, especially at 303 ± 1 K and
18
19 313 pH = 4 respectively.

20 21 22 314 3.3.2. Dubinin–Radushkevich Isotherm

23
24
25 315 Mean free energy of biosorption is used to describe the nature of biosorption and its mechanism.
26
27
28 316 This mean free energy of biosorption is estimated from the correlation coefficient of Dubinin–
29
30 317 Radushkevich isotherm. The D–R isotherm model was well fitted to the equilibrium data since
31
32 318 R^2 values were found to be 0.998 for arsenic (Fig. (6c)). From the intercept of the plot, the q_m
33
34 319 value was found to be 18.919×10^{-2} mg/g for arsenic. The mean biosorption energy was measured
35
36
37 320 as 5.79 kJ/mol for arsenic. This result suggests that the bio-sorption of arsenic onto *T. vulgaris*
38
39 321 might take place via chemical reaction involving valence forces through sharing or exchange of
40
41
42 322 electrons between sorbent and sorbate.

43 44 323 3.3.3. Temkin isotherm

45
46
47 324 Temkin and Pyzhev revealed the effects of indirect adsorbate/adsorbate interactions on
48
49 325 biosorption isotherms. Due to adsorbate/adsorbate interactions the heat of biosorption of all the
50
51 326 molecules in the layer would decrease linearly with coverage [20].
52
53
54
55
56
57
58
59
60

1
2
3 327 The biosorption data of arsenic onto *T.vulgaris* was investigated according to the linear form of
4
5 328 the Temkin isotherm and the resultant graph represented in Fig. (6d). The examined data shows
6
7 329 that the Temkin isotherm provides a close fit to the arsenic biosorption onto *T.vulgaris*. The
8
9 330 linear isotherm constants and coefficients of determination are shown in Table 4.

10
11
12
13 331 The equilibrium sorption data of arsenic onto *T. vulgaris* was fitted well to all four
14
15 332 equilibrium models and estimated isotherm constants are displayed in Table 4. Based on the
16
17 333 linear regression correlation coefficient (R^2), best fitted equilibrium model was established. The
18
19 334 corresponding Table 4 displays that sorption data of arsenic were extremely well classified by
20
21 335 Langmuir isotherm with higher correlation coefficient of 0.999, followed by Dubinin–
22
23 336 Radushkevich, Temkin and Freundlich isotherm with a value of 0.998, 0.996 and 0.971
24
25 337 respectively. The higher biosorption capacity Q_{\max} indicates the strong electrostatic force of
26
27 338 attraction.

339 3.4. Kinetic studies

34
35 340 Biosorption kinetics study illustrates the solute uptake rate, which in turn governs the residence
36
37 341 time of biosorption. Hence, kinetic study of removal of arsenic using biosorbent was carried out
38
39 342 with different initial arsenic concentrations ranging from 20–100 mg/l at an initial pH of 4 and
40
41 343 temperature of 303 K. The suitability of kinetic data to pseudo first and second order rate
42
43 344 equations is described in Figs. (7a) and (7b) and corresponding rate constants, predicted arsenic
44
45 345 uptake and R^2 values are reported in Table 5. In case of pseudo first order model R_1^2 values were
46
47 346 found in the range of 0.958–0.982 which shows the significance of model, but the predicted
48
49 347 maximum metal uptake values were expressively differed with the experimental values.
50
51 348 According to Sinha et al. [21], if the predicted metal uptake is not equal to experimental value
52
53 349 the kinetic equation is not appropriate, even if the plot has a high regression coefficient. Hence

1
2
3 350 pseudo first order rate equation is not suitable for kinetics determination. In case of pseudo
4
5 351 second order, high correlation coefficients and nearer predicted and experimental metal uptake
6
7 352 values indicates the model significance of biosorption kinetics of arsenic. Therefore biosorption
8
9
10 353 of arsenic onto *T.vulgaris* follows pseudo second order model along with chemisorption as a rate
11
12 354 determining step [22]. Further kinetic data were fitted to Elovich model to confirm the
13
14 355 chemisorption. As shown in Fig. (8c) the plots are linear with good correlation coefficient (R^2 in
15
16 356 the range of 0.985). So the suitability of data to Elovich model suggests the biosorption of
17
18 357 arsenic follows chemisorption, involving valence forces through sharing or exchange of electrons
19
20 358 between biosorbent and biosorbate [23]. The rate constant (k_2) values were decreased from 0.052
21
22 359 to 0.006 1/ g min with an increase in initial arsenic ion concentration where as the initial sorption
23
24 360 rate increased from 1.186 to 4.201 mg/g min which shown in Table 5. This can be interpreted as
25
26 361 with an increase in initial metal concentration, concentration gradient increases between bulk
27
28 362 solution and biosorbent surface, results the driving force for metal uptake. However at higher
29
30 363 concentrations, greater probability of metal ion collisions makes metal ions diffusion towards the
31
32 364 surface ligands or micro pores difficult and hence reduces the overall rate of kinetics. The intra-
33
34 365 pore diffusion of arsenic ion is investigated by fitting the kinetic data to intra particle diffusion
35
36 366 model. Fig. (8a) shows the fitness of kinetic data to the intraparticle diffusion model. If the intra-
37
38 367 particle diffusion is the only rate-controlling step then the plot should pass through the origin,
39
40 368 else the boundary layer diffusion affects the biosorption to some degree. From Fig. (8a) it was
41
42 369 clear that the linear curves are not passing through the origin which indicates the existence of
43
44 370 external pore diffusion in biosorption. Similar trend was reported by Jafari et al. [24] for
45
46 371 biosorption of arsenic onto brown seaweed and by Ofomaja [25] for removal of lead using
47
48 372 mansonia wood sawdust. Further investigation was performed towards the kinetic data matching
49
50
51
52
53
54
55
56
57
58
59
60

1
2
3 373 with Boyd model to observe an exact rate limiting step and calculated B_t values then plotted
4
5 374 against contact time. From the linear trend the rate controlling step of biosorption can be
6
7
8 375 obtained. If the plot is linear and passes through the origin, the pore diffusion is the rate
9
10 376 controlling step otherwise surface (film) diffusion indicates the rate limiting stage. Fig. (8b)
11
12 377 represents the plot of B_t vs contact time which was linear with correlation coefficient ($R^2 =$
13
14 378 0.696), but it was not passed through the origin, indicates the external mass transport controlled
15
16
17 379 process, where particle diffusion is rate determining step.

20 380 **4. Conclusion**

21
22
23 381 The chemically modified biosorbent prepared from the biomass of *T.vulgaris* towards the
24
25 382 removal of arsenic (As) from aqueous metal solutions was investigated and the biosorption
26
27 383 potential of prepared bio-sorbent was optimized with the help of RSM software. The surface
28
29
30 384 functional groups responsible for biosorption of arsenic onto *T. vulgaris* were identified using
31
32 385 FTIR and found that carboxylic acids, amino, alkenes and alkyl groups are involved in metal
33
34
35 386 binding. The surface texture and porosity of the biosorbent was analyzed by SEM analysis and
36
37 387 found that the biosorbent surface is highly heterogeneous and uneven with porous structure. The
38
39 388 maximum theoretical arsenic biosorption potential was estimated to be 26.54 mg/g, which is
40
41 389 fairly high compared to previous reports. Further behaviour of arsenic biosorption onto *T.*
42
43
44 390 *vulgaris* was investigated through kinetic studies and results illustrated chemisorption with
45
46 391 surface ions exchange. The present study concludes that bio-sorbent produced from *T.vulgaris*
47
48 392 could be a potential sorbent towards the removal of metal arsenic.

51 393 **Acknowledgement**

52
53
54 394 The authors would like to acknowledge Vignan's Foundation for Science, Technology &
55
56 395 Research Deemed to be University for providing facilities to carry the research work.

396 **References**

- 397
- 398 1. Ungureanu, G., Santos, S., Boaventura, R., & Botelho, C. (2015). Arsenic and antimony
399 in water and wastewater: overview of removal techniques with special reference to latest
400 advances in adsorption, *J. Environ. Manage*, 151, 326-342.
- 401 2. Srivastava, S., & Dwivedi, A.K. (2015). Biological wastes the tool for biosorption of
402 arsenic, *J Bioremed & Biodeg*, 7, 323.
- 403 3. Zeraatkar, A.K., Ahmadzadeh, H., Talebi, A.F., Moheimani, N.R., & McHenry,
404 M.P.(2016). Potential use of algae for heavy metal bioremediation, a critical review, *J.*
405 *Environ. Manage*, 181, 817-831.
- 406 4. Ibrahim, W.M. (2011). Biosorption of heavy metal ions from aqueous solution by red
407 macroalgae, *J. Hazard. Mater.*, 192(3), 1827-1835.
- 408 5. Bulgariu, D., & Bulgariu, L. (2012). Equilibrium and kinetics studies of heavy metal ions
409 biosorption on green algae waste biomass, *Bioresour. Technol*, 103(1), 489-493.
- 410 6. Sulaymon, A.H., Mohammed, A.A., & Al-Musawi T.J. (2013). Competitive biosorption
411 of lead, cadmium, copper, and arsenic ions using algae, *Environ. Sci. Pollut. Res*, 20(5),
412 3011-3023.
- 413 7. Banerjee, S., Banerjee, A., Sarkar., & P. (2018). Statistical optimization of arsenic
414 biosorption by microbial enzyme via Ca-alginate beads, *J. Environ. Sci. Health., Part*
415 *A*, 53(5), 436-442.
- 416 8. Prasad, K.S., Ramanathan, A.L., & Paul, J., V. Subramanian, R. Prasad.(2013).
417 Biosorption of arsenite (As⁺³) and arsenate (As⁺⁵) from aqueous solution by
418 *Arthrobacter* sp. Biomass, *ENVIRON TECHNOL*, 34(19), 2701-2708.
- 419 9. Kwak, H.W., Kim, M.K., Lee, J.Y., Yun, H., Kim, M.H., Park, Y.H., & Lee, K.H.,
420 (2015). Preparation of bead-type biosorbent from water-soluble *Spirulina platensis*
421 extracts for chromium (VI) removal, *Algal Research*, 7, 92-99.
- 422 10. Baig, J.A., Kazi, T.G., Shah, A.Q., Kandhro, G.A., Afridi, H.I., Khan, S., & Kolachi,
423 N.F. (2010). Biosorption studies on powder of stem of *Acacia nilotica*: removal of arsenic
424 from surface water, *J. Hazard. Mater*, 178(1-3), 941-948.
- 425 11. Srivastava, S., Agrawal, S.B., & Mondal, M.K.(2015). Biosorption isotherms and kinetics
426 on removal of Cr (VI) using native and chemically modified *Lagerstroemia speciosa*

- 1
2
3 427 bark, *Ecol. Eng.*, 85, 56-66.
- 4
5 428 12. Jerold , M., & Sivasubramanian, V.(2016). Biosorption of malachite green from aqueous
6
7 429 solution using brown marine macro algae *Sargassum swartzii*, *Desal. Water*
8
9 430 *Treat.*, 57(52), 25288-25300..
- 10 431 13. Babu, D. J., Sumalatha, B., Venkateswarulu, T.C., Das, K. M., & Kodali, V. P. (2014).
11
12 432 Kinetic, Equilibrium and Thermodynamic Studies of Biosorption of Chromium (VI) from
13
14 433 Aqueous Solutions using *Azolla filiculoides*, *J PURE APPL MICROBIO*, 8, 3107-3116.
- 15 434 14. Tafakori, V., Zadmard, R., Tabandeh, F., Amoozegar, M.A., & Ahmadian, G. (2017).
16
17 435 Equilibrium Isotherm, Kinetic Modeling, Optimization, and Characterization Studies of
18
19 436 Cadmium Adsorption by Surface-Engineered *Escherichia coli*, *Iranian biomedical*
20
21 437 *journal*, 21(6), 380.
- 22 438 15. Ananta,S., Saumen, B., & Vijay,V.(2015). Adsorption isotherm, thermodynamic and
23
24 439 kinetic study of arsenic (III) on iron oxide coated granular activated charcoal, *Int. Res. J.*
25
26 440 *Environment Sci.*, (1), 4, 64-77.
- 27 441 16. Shafique, U., Ijaz, A., Salman, M., M., uz Zaman W. , Jamil, N., Rehman, R., & Javaid,
28
29 442 A.(2012). Removal of arsenic from water using pine leaves, *Journal of the Taiwan*
30
31 443 *Institute of Chemical Engineers*, 43(2), 256-263.
- 32 444 17. Pagnanelli, F., Mainelli, S., Vegliò, F., & Toro, L.(2003). Heavy metal removal by olive
33
34 445 pomace: biosorbent characterisation and equilibrium modelling, *Chem. Eng. Sci.*, 58,
35
36 446 4709–4717.
- 37 447 18. John Babu,D., Sumalatha, B., King, Pulipati, & Prasanna Kumar Yekula. (2018).
38
39 448 Investigation on biosorption of Cd(II) onto *Gelidiella acerosa*(brown algae):
40
41 449 Optimization(using RSM &ANN) and mechanic studies, *Desal. Water Treat.*, 107, 195-
42
43 450 206.
- 44 451 19. Sugashini, S., & Begum, K.M.S. (2013). Optimization using central composite design
45
46 452 (CCD) for the biosorption of Cr (VI) ions by cross linked chitosan carbonized rice husk
47
48 453 (CCACR), *Clean Techn. Environ. Policy*, 15, 293–302.
- 49 454 20. Javanbakht, V., & Ghoreishi, S.M. (2017). Application of response surface methodology
50
51 455 for optimization of lead removal from an aqueous solution by a novel super paramagnetic
52
53 456 nanocomposite, *Adsorpt. Sci. Technol.*, 35(1-2), 241-260.
- 54
55 457 21. Indhumathi, P., Syed Shabudeen, P.S., Shoba, U.S., Saraswathy, & C.P. (2014). The

- 1
2
3 458 removal of chromium from aqueous solution by using green micro algae, Journal of
4 Chemical and Pharmaceutical Research, 6(6), 799-808.
5 459
6
7 460 22. Lodeiro, P., Barriada, J.L., Herrero, R., & De Vicente, M.S.(2006). The marine
8 461 macroalga *cystoseira baccata* as biosorbent for cadmium (II) and lead (II) removal:
9 kinetic and equilibrium studies, *Environ. Pollut.*, 142, 264–273.
10 462
11
12 463 23. Kumar, P.S., Ramalingam, S., Kirupha, S.D., Murugesan, A., Vidhyadevi, & Sivanesan,
13 464 T., S. (2011). Adsorption behavior of nickel (II) onto cashew nut shell: Equilibrium,
14 thermodynamics, kinetics, mechanism and process design. *Chem. Eng. J.*, 167,122–131.
15 465
16
17 466 24. Jafari, S.A., Jamali, A., Hosseini, A. (2010). Cadmium removal from aqueous solution
18 467 by brown seaweed, *Sargassum angustifolium*, *Korean J. Chem. Eng.*, 32, 2053–2066.
19
20 468 25. Ofomaja, A.E. (2010). Intra particle diffusion process for lead (II) biosorption onto
21 469 *mansonia wood sawdust*, *Bioresour. Technol.*, 101, 5868–5876.
22
23
24
25
26
27
28
29
30
31
32
33
34
35
36
37
38
39
40
41
42
43
44
45
46
47
48
49
50
51
52
53
54
55
56
57
58
59
60

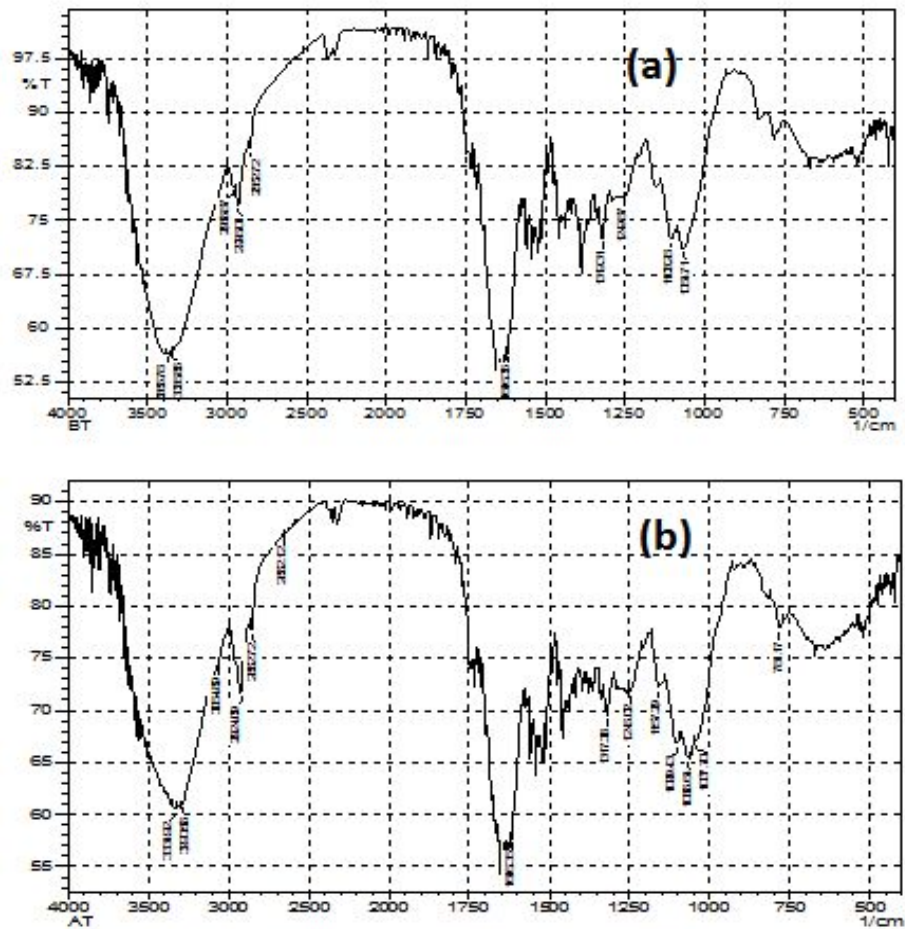


Fig 1 FTIR spectra of *T. vulgaris* a) before biosorption b) after biosorption

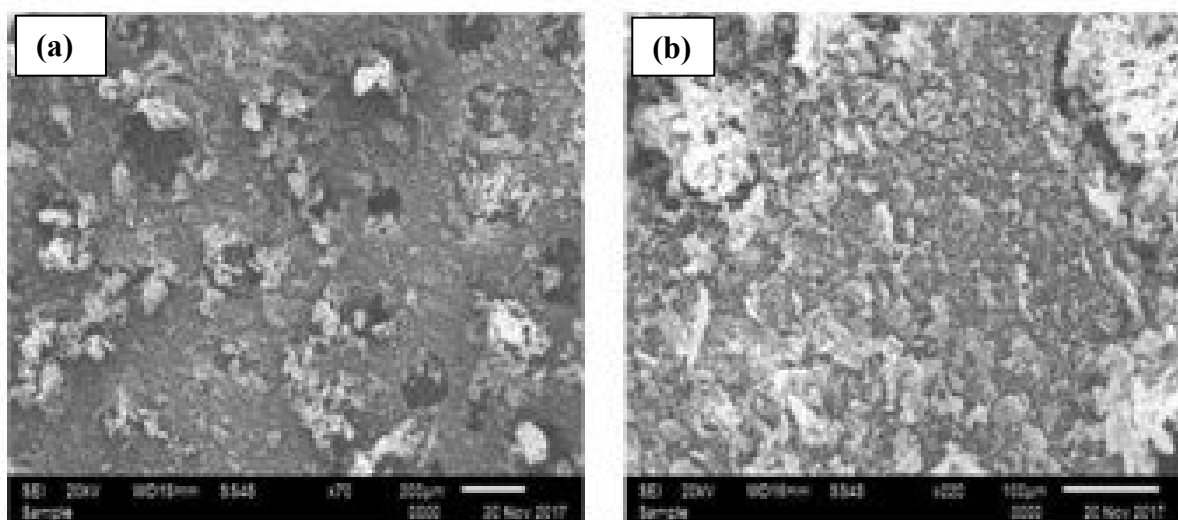


Fig. 2 SEM analysis for biosorption of arsenic using *T. vulgaris* a) before and b) after biosorption

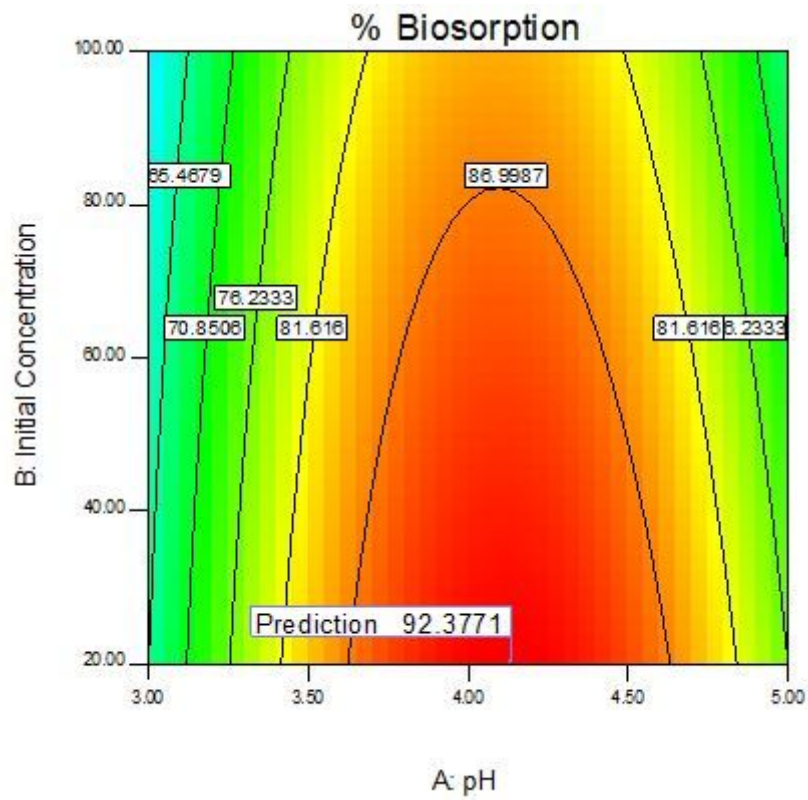


Fig 3 Contour plot of optimization of biosorption of arsenic onto *T. Vulgaris*.

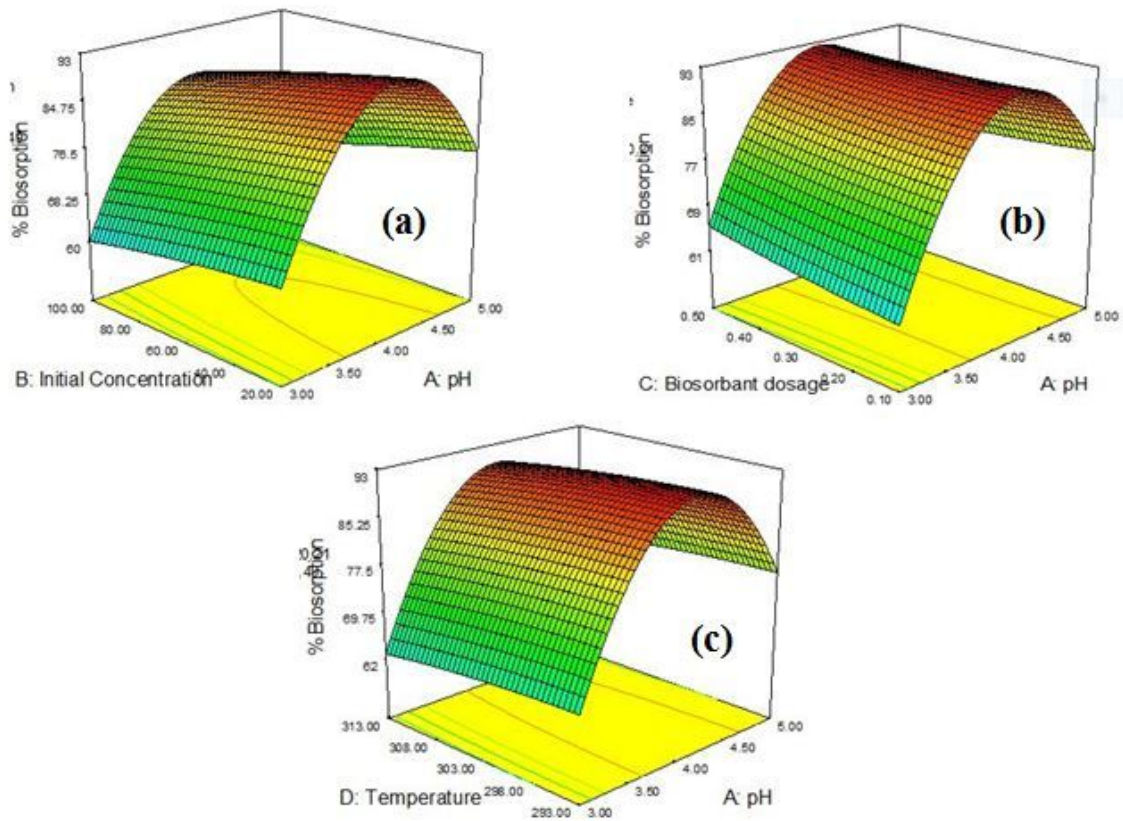


Fig. 4 Response surface plot for interactive effects of (a) initial concentration and pH, (b) biosorbent dosage and pH, (c) temperature and pH on biosorption of arsenic using modified *T. vulgaris* as biosorbent.

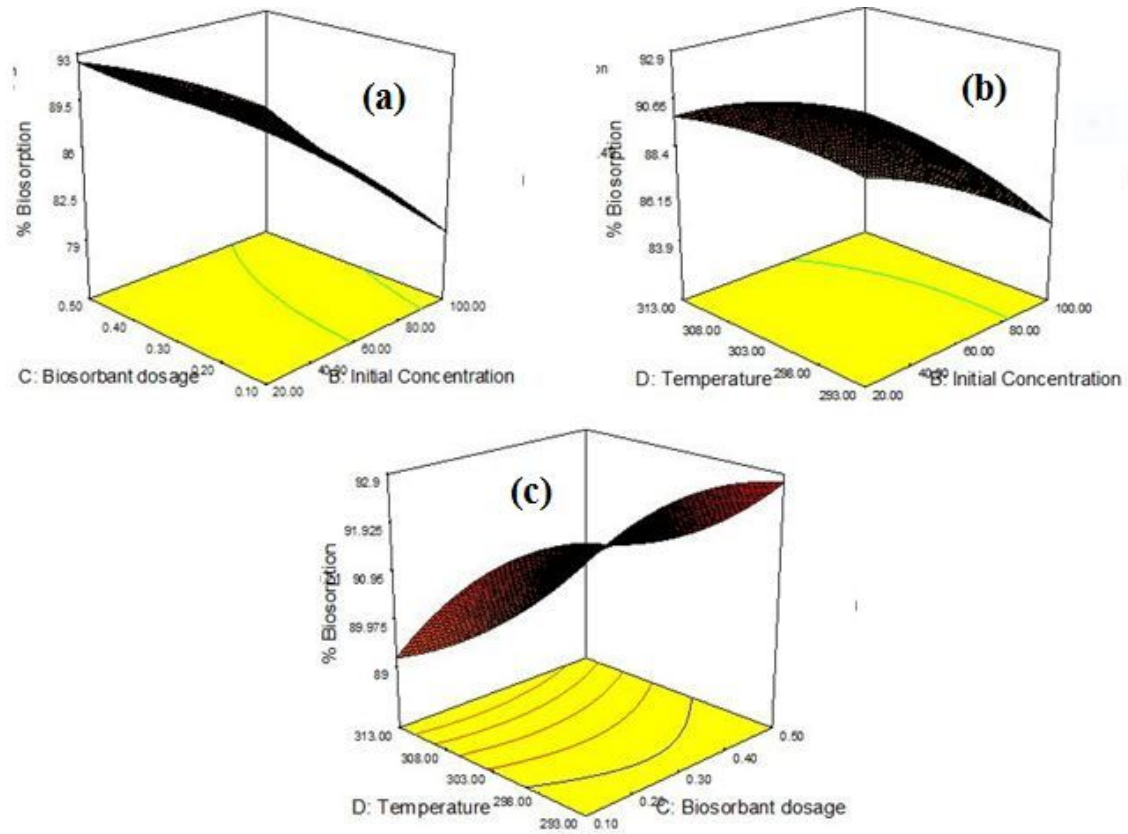


Fig. 5 Response surface plot for interactive effects of (a) biosorbent dosage and initial concentration, (b) temperature and initial concentration, (c) temperature and biosorbent dosage on biosorption of arsenic using modified *T. vulgaris* as biosorbent.

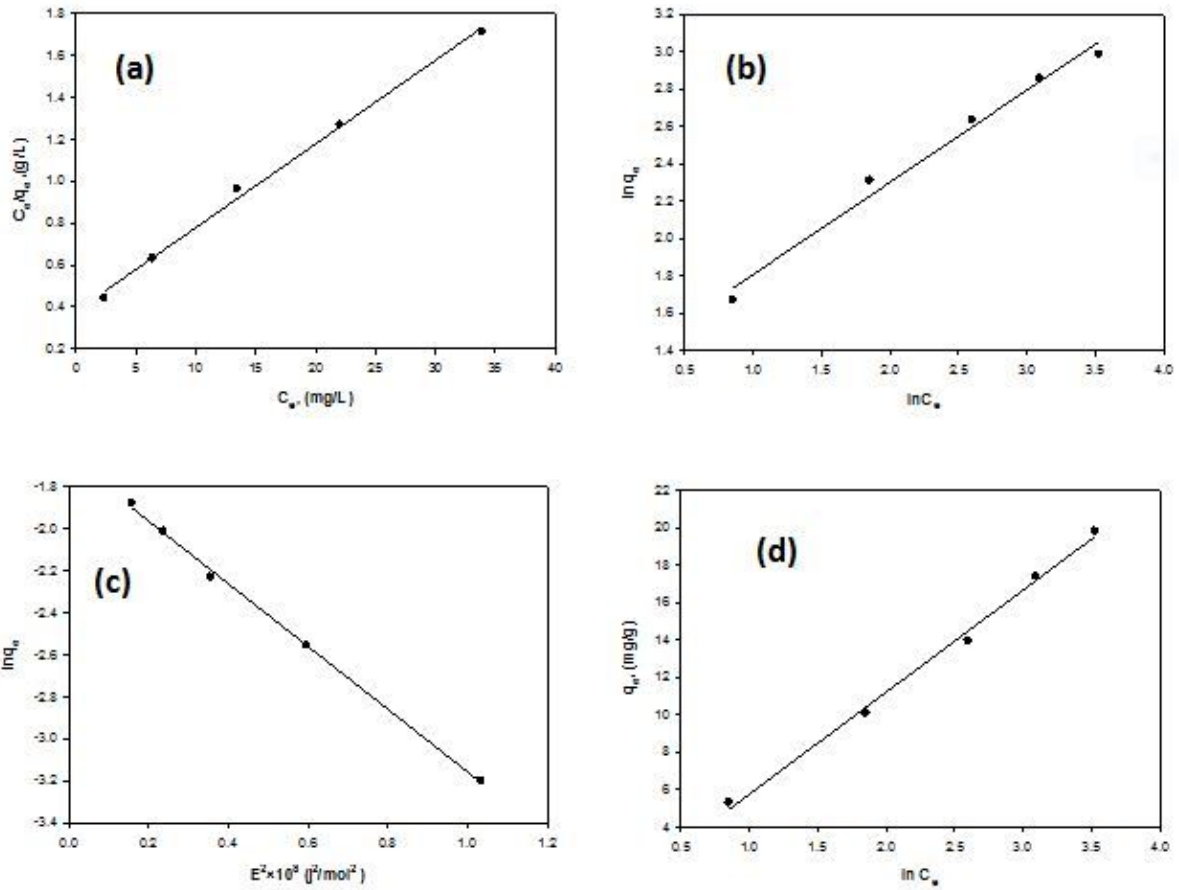


Fig. 6 a) Langmuir b) Freundlich c) D-R d) Temkin isotherm models for biosorption of arsenic using *T. vulgaris* as biosorbent.

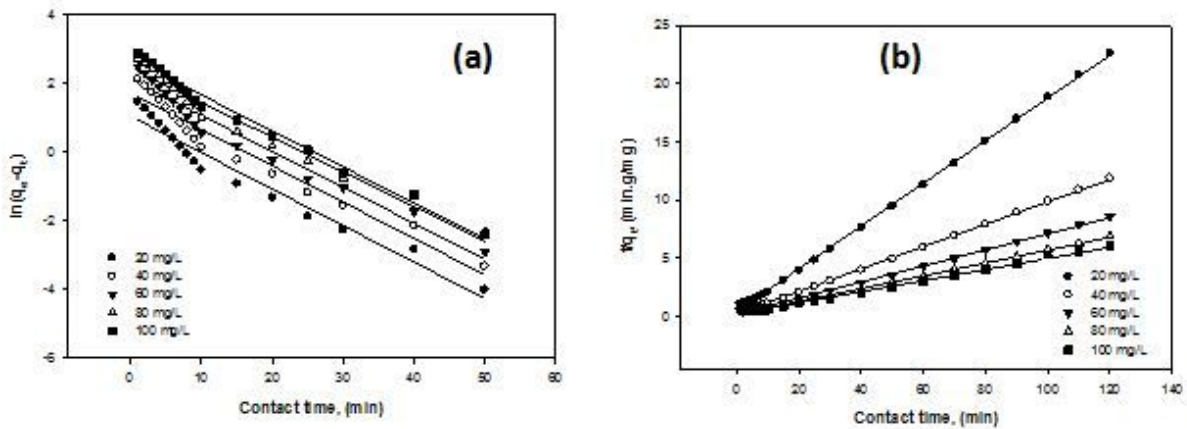


Fig: 7 a) Pseudo first order b) Pseudo second order models for biosorption of arsenic using *T. vulgaris* as biosorbent.

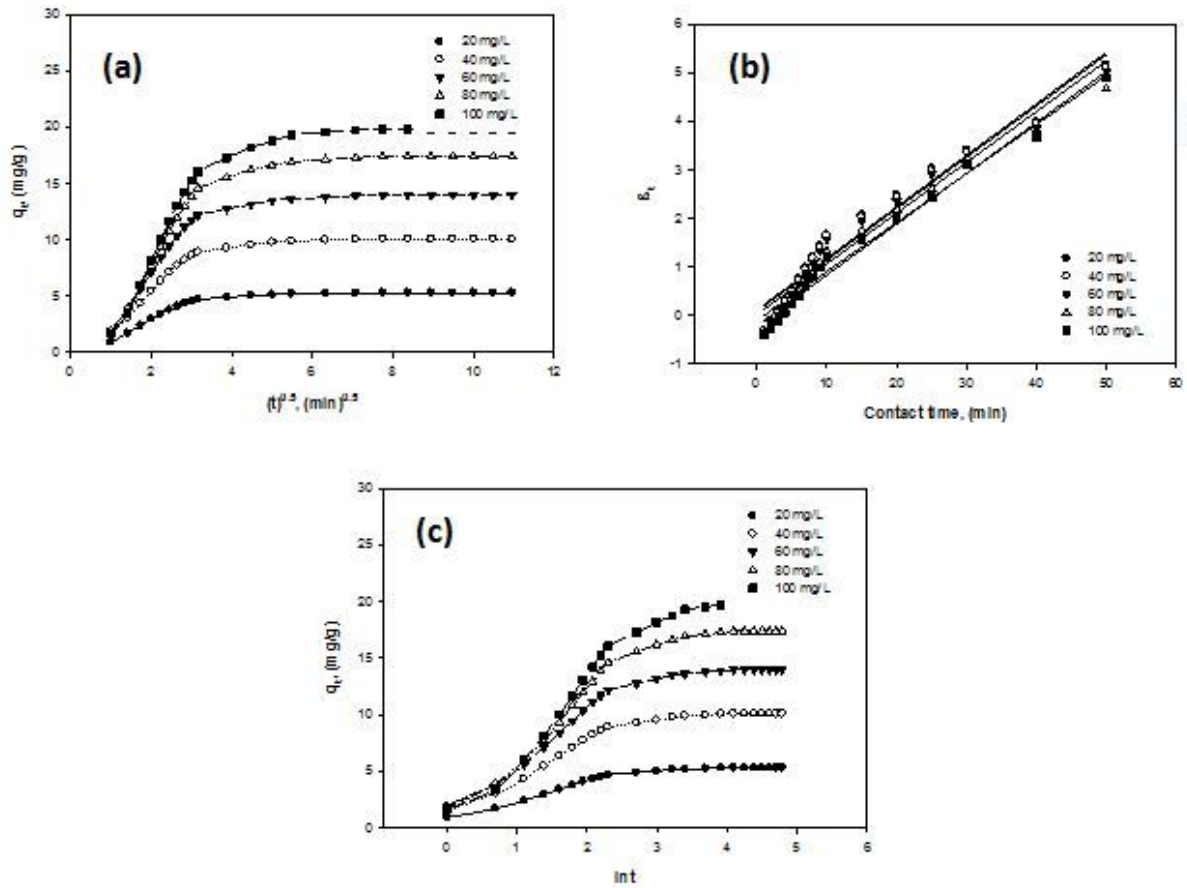


Fig: 8 a) Intra-particle diffusion b) Boyd c) Elovich models for bio-sorption of arsenic using *T. vulgaris* as biosorbent.

Table 1 Levels of different process variables used in CCD for bio-sorption of arsenic onto *T. vulgaris*.

Factor	Name	Units	Symbol & levels		
			-1	0	1
A	pH	--	3.00	4.000	5.00
B	Initial arsenic concentration	mg/l	20.00	60.000	100.00
C	<i>T. vulgaris</i> dosage	G	0.100	0.300	0.50
D	Temperature	K	293.00	303.000	313.00

Table 2 Experimental design (CCD) observed and predicted response for biosorption of arsenic onto *T. vulgaris*.

Standard order	pH	Initial concentration	Biosorbent dosage	Temperature	Experimental % biosorption	Predicted % biosorption
1	3.00	20.00	0.10	293.00	61.64	62.03
2	5.00	20.00	0.10	293.00	80.28	79.42
3	3.00	100.00	0.10	293.00	51.58	51.11
4	5.00	100.00	0.10	293.00	64.51	64.79
5	3.00	20.00	0.50	293.00	65.23	65.82
6	5.00	20.00	0.50	293.00	76.19	76.53
7	3.00	100.00	0.50	293.00	60.37	60.10
8	5.00	100.00	0.50	293.00	67.62	67.10
9	3.00	20.00	0.10	313.00	58.24	58.49
10	5.00	20.00	0.10	313.00	75.41	75.92
11	3.00	100.00	0.10	313.00	49.64	49.53
12	5.00	100.00	0.10	313.00	64.1	63.24
13	3.00	20.00	0.50	313.00	63.04	62.99
14	5.00	20.00	0.50	313.00	73.54	73.74
15	3.00	100.00	0.50	313.00	58.64	59.23
16	5.00	100.00	0.50	313.00	66.42	66.26
17	3.00	60.00	0.30	303.00	60.22	59.29
18	5.00	60.00	0.30	303.00	70.43	71.50
19	4.00	20.00	0.30	303.00	92.12	90.74
20	4.00	100.00	0.30	303.00	80.03	81.54
21	4.00	60.00	0.10	303.00	84.49	85.34
22	4.00	60.00	0.50	303.00	89.45	88.74
23	4.00	60.00	0.30	293.00	86.67	87.18
24	4.00	60.00	0.30	313.00	85.37	84.99
25	4.00	60.00	0.30	303.00	87.95	86.63
26	4.00	60.00	0.30	303.00	86.28	86.63
27	4.00	60.00	0.30	303.00	85.94	86.63
28	4.00	60.00	0.30	303.00	87.04	86.63
29	4.00	60.00	0.30	303.00	86.24	86.63
30	4.00	60.00	0.30	303.00	86.73	86.63

Table 3 ANOVA for quadratic surface model for biosorption of arsenic onto *T. vulgaris*.

Source	Sum of Squares	df	Mean Square	F Value	p-value Prob > F	
Model	4603.30	14	328.81	352.88	< 0.0001	Significant
<i>A-pH</i>	671.00	1	671.00	720.12	< 0.0001	
<i>B-Initial Concentration</i>	380.70	1	380.70	408.57	< 0.0001	
<i>C-Biosorbant dosage</i>	52.05	1	52.05	55.86	< 0.0001	
<i>D-Temperature</i>	21.54	1	21.54	23.12	0.0002	
<i>AB</i>	13.78	1	13.78	14.79	0.0016	
<i>AC</i>	44.59	1	44.59	47.85	< 0.0001	
<i>AD</i>	1.056E-003	1	1.056E-003	1.134E-003	0.9736	
<i>BC</i>	27.01	1	27.01	28.99	< 0.0001	
<i>BD</i>	3.83	1	3.83	4.11	0.0607	
<i>CD</i>	0.51	1	0.51	0.54	0.4718	
<i>A²</i>	1168.58	1	1168.58	1254.12	< 0.0001	
<i>B²</i>	0.62	1	0.62	0.66	0.4290	
<i>C²</i>	0.43	1	0.43	0.46	0.5071	
<i>D²</i>	0.76	1	0.76	0.82	0.3800	
Residual	13.98	15	0.93			
<i>Lack of Fit</i>	11.33	10	1.13	2.14	0.2071	not significant
<i>Pure Error</i>	2.64	5	0.53			
Cor Total	4617.28	29				

Table 4 Equilibrium constants for biosorption of arsenic onto *T. vulgaris*

Isotherm	Constants	Arsenic
Langmuir	Q_{\max} (mg / g)	25.64
	K_L (L / mg)	0.102
	R^2	0.996
Freundlich	K_f (mg / g)	3.724
	$1/n$ (L / g)	0.493
	R^2	0.984

Temkin	$A_T (L / mg)$	4.845
	b_T	0.057
	R^2	0.995
Dubinin– Radushkevich	$Q_{\max} (mg / g)$	18.919×10^{-2}
	β	1.491×10^{-8}
	$E (kJ / mol)$	5.79
	R^2	0.998

Table 5 Pseudo first & second order kinetic constants for biosorption of arsenic onto *T. vulgaris*

Initial concentration, mg/L	First order			Second order		
	Rate constant, k_1 (1/ min)	Amount of arsenic biosorbed onto <i>T. vulgaris</i> , q_{eq} (mg/g)	Correlation coefficient, R_1^2	Rate constant, k_2 (g / mg min)	Amount of arsenic biosorbed onto <i>T. vulgaris</i> , q_{eq} (mg/g)	Correlation coefficient, R_2^2
20	0.106	2.880	0.958	0.0715	5.464	0.999
40	0.105	5.663	0.958	0.0349	10.4166	0.999
60	0.122	9.355	0.974	0.022	14.4927	0.998
80	0.101	11.763	0.967	0.013	18.5185	0.998
100	0.104	15.256	0.982	0.0091	21.2765	0.994

Table 6 Comparison of the arsenic biosorption capacity of present work with those reported in the literature

Adsorbent/Biosorbent	q_{\max} (mg/g)	Reference
<i>Lessonia nigrescens</i>	4.2	26
Activated <i>Moringa oleifera</i>	6.23	27
shelled <i>Moringa oleifera</i> Lamarck seedpowder	2.16	28
powder of stem of <i>Acacia nilotica</i>	5.8	29
untreated powdered eggshell	2.14	30
Use of fly ash and fly ash agglomerates	5.7	31
Coagulant Of Plant Origin With Ferric Chloride	1.38	32
AC (olive pulp)	1.39	33
<i>Turbinaria vulgaris</i> sp.	25.64	Present study